Analytical Science Advances

WILEY-VCH

Chemistry Europe
European Chemical Societies Publishing

RESEARCH ARTICLE OPEN ACCESS

Bioactive Potential of the Sulfated Exopolysaccharides From the Brown Microalga *Halamphora* sp.: Antioxidant, Antimicrobial, and Antiapoptotic Profiles

Fatma Ben Mansour[1] | Wassim Guermazi[1] | Mohamed Chamkha[2] | Khaled Bellassoued[3] | Hichem Ben Salah[4] | Abdel Halim Harrath[5] | Waleed Aldahmash[5] | Md Ataur Rahman[6] | Habib Ayadi[1]

[1]Department of Life Sciences, Laboratory of Marine Biodiversity and Environment, Faculty of Sciences, University of Sfax, Sfax, Tunisia | [2]Laboratory of Environmental Bioprocesses, Centre of Biotechnology of Sfax, University of Sfax, Sfax, Tunisia | [3]Department of Life Sciences, Animal Ecophysiology Laboratory, University of Sfax, Sfax, Tunisia | [4]Department of Life Sciences, Laboratory of Organic Chemistry LR17ES08 (Natural Substances Team), Faculty of Sciences of Sfax, University of Sfax, Sfax, Tunisia | [5]Zoology Department, College of Science, King Saud University, Riyadh, Saudi Arabia | [6]Department of Oncology, Karmanos Cancer Institute, Wayne State University, Detroit, Michigan, USA

Correspondence: Habib Ayadi (habibayadi62@yahoo.fr)

Received: 14 July 2024 | **Revised:** 28 August 2024 | **Accepted:** 30 August 2024

Keywords: antiapoptotic | antimicrobial | antioxidant | exopolysaccharides | *Halamphora* sp | microalga

ABSTRACT

This study aims to investigate the physicochemical characteristics of the exopolysaccharides (EPS) extracted from the microalgae species *Halamphora* sp., as well as to evaluate their antioxidant, antibacterial, and anti-apoptotic activities. The crude extracellular polysaccharides from the halophilic diatom *Halamphora* sp. were found to be extracellular heterosulfated anionic polysaccharides containing carbohydrates (76.33 ± 1.80%), proteins (0.15 ± 0.02%), uronic acids (5.44 ± 0.08%) and sulfate (7.56 ± 0.86%). The lowest protein (0.24%) and lipid (0.15%) contents suggested that EPS was highly pure. Gas chromatography–mass spectrometry analysis revealed that the carbohydrate fraction consisted of xylose, L-galactose, D-galactose, glucose, ribitol, mannose, and inositol with corresponding mole percentages of 40.55, 13.25, 13.00, 9.95, 9.82, 2.90, and 2.28, respectively. In vitro, tests showed a high total antioxidant capacity probably related to L-galactose followed by D-galactose, uronic acid, and ribitol. In addition, extracellular polysaccharides (EPS) demonstrated effective antimicrobial Gram + properties with inhibition zones ranging from 10 to 12 mm. Molecular docking showed an antiapoptotic effect, as the best docking score was generated due to the interaction of xylose and caspase 3 (−6.9 kcal/mol) and L-galactose and caspase 3 (−5 kcal/mol). Overall, the findings of this study suggest the possibility of using the EPS extract of *Halamphora* sp. as an additive for nutraceutical and cosmetic purposes.

1 | Introduction

Primary metabolism macromolecules, such as monosaccharides, exopolysaccharides, lipids, and proteins are found in every organism, but the distribution of secondary metabolism is more restricted [1]. The production is caused by particular organisms or a group of extremophile organisms living in extreme conditions, such as temperature, pH, and salinity. In fact, organisms produce large compounds of bioactive interest to protect themselves or to play an important role in their daily life within their living

Fatma Ben Mansour and Wassim Guermazi contributed equally to this study.

ecosystem. This shows that bioactive molecules are present in unrelated biological systems [2]. Recently, halotolerant and halophilic microalgae have been recognized as potential sources of bioactive compounds for nutraceutical applications [3–6].

Microalgae and cyanobacteria are known for their high antioxidant activities due to numerous bioactive substances, including phenolic compounds, lipids [7, 8], carotenoids and proteins [9, 10], phycocyanin [11] and polysaccharides [12, 13]. Among microalgae, diatoms, which produce approximately 25% of the world's primary biomass diatom, produce extracellular polysaccharides (EPS) during their growth, which can constitute 80%–90% of the total extracellular total release [14–17]. Media-soluble polymers that are usually "colloidal carbohydrates" and wall-associated fractions that are usually called "bound carbohydrates" or "extra-cellular matrix (ECM) polymers" are among the extracellular polymers [15, 16]. Diatoms' ability to adapt to their environment involves producing EPS that are primarily composed of sulfated polysaccharides and/or proteoglycans [18]. EPS plays an important ecological role in protecting cells of diatoms from toxic substances and dehydration and acts as energy and carbon sinks during dietary stress. Their roles in forming transparent exopolymeric particles [19], marine gels [20], and biofilms [21] are well recognized and play an important role in regulating sedimentation processes, biogeochemical cycling, and particle dynamics in the oceans via the microbial loop. The formation of algae aggregates is also promoted by EPS, and cell-matrix adhesion is mediated, leading to the stabilizing of the biofilm structure [16]. EPS's commercial attractiveness and growing research focus are due to its potential use in various industries, such as food, medicine, cosmetics, and manufacturing. EPS microalgae were initially used as thickeners and biofat in food products because of their unique physical traits, such as high viscosity and good rheological properties [22, 23]. The physicochemical properties and biological activity of polysaccharides can be influenced significantly by their chemical composition and structural properties. The identification of several types of EPS from microalgae is leading to a gradual diversification of research on their application [24]. Biomass and EPS both have great value as carbon storage for food production. Different microalgae species produce different types of EPS, including sulfated exopolysaccharides, such as *Chlorella stigmatophora*, *Chlorella* sp., *Tetraselmis* sp., *Cylindrotheca closterium*, and *Amphora* sp [25, 26]. In addition, numerous studies, both in vivo and in vitro, have highlighted some of the biological activities of EPS microalgae, such as antibacterial, antioxidant, anti-inflammatory, antiparasitic, immunomodulatory, anticancer, and antithrombotic properties. All these interesting properties (great diversity of microalgae, original structures, physicochemical properties, and/or biological activity) make these organisms attractive for the exploitation of these compounds in different industrial sectors [27]. EPS is usually extracted from the culture medium by alcohol precipitation [27, 28]. Thermal exopolysaccharides are a key feature that opens the possibility of using microalgae exopolysaccharides in food, cosmetic, and pharmaceutical industries [29]. Diatom communities in the Sfax solar saltern are composed of several euryhaline and stenohaline species [30, 31]. Recently, Boukhris et al. [7]. isolated the halophilic diatom *Halamphora* sp. and showed that it is rich in several metabolites, such as lipids, proteins, phenolics, and polysaccharides. This study aims to explore exopolysaccharide extracts from *Halamphora* sp. by investigating their physicochemical properties as well as their antioxidant, antibacterial, and anti-apoptotic activities.

2 | Materials and Methods

2.1 | Microalgae

The bacillariophyceae utilized in this research were recently isolated from a water sample from the saltwork of Sfax in pond C4-1 where the salinity average was 107 p.s.u. The saltwork of Sfax, located in the central-eastern part of Tunisia (34° 39′ N and 10°42′ E), was composed of several interconnected shallow ponds (20–70 cm depth) where the salinity ranged from 40 to 400 p.s.u. [30] The diatom was identified as *Halamphora* sp. using its internal spacer sequence, transcribed from the rDNA sequence (GenBank accession number SB1 MK575516.1).

2.2 | Culture Conditions

Halamphora was grown batch-wise in autoclaved natural seawater enriched by sodium silicate (Na_2SiO_3), and a trace of metal solution according to F/2 medium composition [31, 32]. The salinity of the medium culture was adjusted to 100 p.s.u. *Halamphora*'s cultures were maintained under controlled conditions at 25°C and 60 µmoles photons m^{-2} s^{-1} provided by fluorescent light tube with a light:dark (16 h:8 h) cycle for 15 days.

2.3 | Process of Extraction of Crude Exopolysaccharides

The crude exopolysaccharides (CH-EPS) were isolated from *Halamphora* sp. using the hot water extraction technique according to the method outlined by Sanniyasi et al. [33] The microalgal-filled culture medium was isolated at 12 days and was centrifuged for 20 min at 4000 rpm. Then, the supernatant was separated by filtering through the Whatman No.1 filter paper. The filtrate was incubated at 70°C in boiling water for 40 min. At the same time, the heat-treated aqueous filtrate was mixed with twice the volume of pure ethanol and held overnight at −20°C to enhance precipitation. Subsequently, the centrifugation at 8000 rpm for 5 min yields the precipitated exopolysaccharides in pellet form. Finally, the CH-EPS was dissolved in 1 mL of Milli-Q water and maintained in a hot mantle at 10°C to achieve a dry yield. The yield of extraction was calculated as the percentage of extracted CH-EPS to the total biomass of *Halamphora*.

$$\text{Extraction yield}\,(\%) = (\text{extracted CH} - \text{EPS mass}/\text{total biomass}) \times 100$$

2.4 | CH-EPS Characterization

The amount of total carbohydrate was assessed by the sulfuric acid-phenol colorimetric method using a standard curve generated with glucose as the standard [34]. Furthermore, the protein content was determined by standardizing bovine serum albumin

according to the method of Lowry [35]. Total crude lipids were determined gravimetrically [36]. The total uronic acid content was measured through colorimetry (520 nm) with galacturonic acid as the standard following the method described by Bitter and Muir [37], The concentration of uronic acid in CH-EPS was determined from a standard curve plotted using galacturonic acid as standard. The sulfate content was obtained turbidimetrically as barium sulfate [38]. The sulfated radical content was calculated from a standard curve generated with potassium sulfate as the reference.

2.5 | Chromatographic Analysis

2.5.1 | Acid Hydrolysis

The hydrolysis kinetics is a crucial phase to establish the optimal conditions for releasing simple sugars and oligosaccharides. 50 mg of the CH-EPS extract was hydrolyzed with 2 mL of trifluoroacetic acid (2 M) at 100°C for 5 h in sealed test tubes. Then, the sample was neutralized with NaOH (1 M) and subsequently centrifuged at 2000 × *g* for 5 min. The supernatant was collected and analyzed using gas chromatography–mass spectrometry (GC–MS).

2.5.2 | Gas Chromatography-MS

The neutral sugar composition was analyzed using GC–MS, a standard method for determining the composition of exopolysaccharides, including the types and molar ratios of monosaccharides. This analysis was conducted following the hydrolysis of the exopolysaccharides from *Halamphora* sp. as described earlier. The exopolysaccharides solution was performed on an HP 5890 Series II GC chromatograph coupled to an HP 5970 mass spectrometer (Amsterdam, The Netherlands) equipped with a DB-225MS (Durabond) fused silica capillary column (30 m × 0.25 mm). The temperature gradient across the column was adjusted starting at 180°C to rise 280°C at 5°C/min. The inlet and detector were maintained at 280°C. Helium was used as a carrier gas with a flow rate set at 1 mL/min.

2.6 | Structural Analysis of CH-EPS

2.6.1 | Fourier Transform Infrared Spectrum

The structural groups present in the CH-EPS extracted from *Halamphora* sp. were carried out by a Fourier-transform infrared spectrum (FTIR) spectrometer (Nicolet) equipped with a horizontally attenuated total reflectance accessory. One milligram of dried CH-EPS was mixed with KBr powder, ground together, and then compressed into 1 mm pellets for FTIR measurement from 4000 to 400 cm^{-1}. The spectroscopy results were analyzed using the software OPUS 3.0 (Bruker).

2.6.2 | Nuclear Magnetic Resonance Spectroscopy

The structure CH-EPS was determined using ^{1}H and ^{13}C NMR Bruker 600 MHz spectrometer at 25°C. Thirty milligrams of dry CH-EPS were dissolved in 1 mL of deuterium oxide (99.9%). ^{1}H and ^{13}C NMR spectra were recorded at the two spectrometer frequencies 300 and 75.5 MHz, respectively. The data analysis was conducted using MestReNova 5.3.0 software (Mestrelab Research S.L.). Chemical shifts corresponding to the location of the signal in the nuclear magnetic resonance (NMR) spectrum are expressed in parts per million.

2.7 | Assessment of Antioxidant Activities

The antioxidant properties of the CH-EPS extracted from *Halamphora* sp. were assessed through in vitro tests.

2.7.1 | Determination of Total Antioxidant Capacity

The test depends on the ability of CH-EPS to reduce Mo(VI) to Mo(V) under acidic pH conditions, leading to the creation of a green phosphate/Mo(V) complex [39]. Aliquots of CH-EPS were mixed with 1 mL of a reagent solution containing 4 mM ammonium molybdate, 28 mM sodium phosphate, and 0.6 M sulfuric acid in an Eppendorf tube. Samples were maintained in a heating block at 95°C for 90 min. Once the mixture had cooled to room temperature, the absorbance of each solution was measured at 695 nm. Total antioxidant capacity (TAC) was expressed in mg vitamin C equivalent/g of sample. Each sample was analyzed three times.

2.7.2 | Measurement of Free Radical-Scavenging Activity

Free radical scavenging activity of CH-EPS was assessed spectrophotometrically at 517 nm against the indicator 2,2-diphenyl-1-picrylhydrazyl (DPPH) [40]. The control is vitamin C was used as a standard. The antioxidant scavenging activity of CH-EPS was expressed as a percentage of DPPH absorbance and calculated using the following equation:

$$\%\text{DPPH scavenging} = [(A0 - A1)/A0] \times 100$$

where A0 = the absorbance of the control reaction and A1 = the absorbance in the presence of CH-EPS triplicate analyses were conducted for each sample.

2.7.3 | Hydroxyl Radical Scavenging Activity Test

The ability of CH-EPS to scavenge hydroxyl radical was assessed using the method outlined by [41] with minor modifications. The reaction mixture consisted of deoxyribose (2.8 mM), KH_2PO_4—NaOH buffer at pH 7.4 (0.05 M), EDTA (0.1 mM), $FeCl_3$ (0.1 mM), H_2O_2 (1 mM), and different concentrations of CH-EPS in a final volume of 2 mL. The mixture was incubated at 37°C for 30 min, followed by 2 mL of trichloroacetic acid (2.8% w/v) and thiobarbituric acid were added. Subsequently, the mixture was subjected to boiling water for 30 min. Once the mixture was cooled the absorbance was measured at 532 nm using an ultraviolet-visible spectrophotometer, with vitamin C serving as control. The following equation was computed to calculate the

percentage of hydroxyl radical scavenged by CH-EPS.

$$\text{Hydroxyl radical scavenging ability (\%)} = [A0 - (A1 - A2)] \times 100/A0$$

A0 represents the absorbance of the control without a sample, A1 is the absorbance after the addition of the sample and 2-deoxy-D-ribose, and A2 is the absorbance of the sample without 2-deoxy-D-ribose. The measurement was done in triplicate for each concentration.

2.7.4 | Superoxide Radical Scavenging Activity Assay

Inhibition of nitrotetrazolium blue (NBT) reduction caused by photochemically generated O_2^- was used to determine the scavenging activity of *CH-EPS* on superoxide anion [42]. Vitamin C served as the reference standard. The percentage of superoxide anion inhibited by CH-EPS was determined as follows:

$$\%\text{superoxide anion scavenging} = [(A0 - A1)/A0] \times 100$$

where A0 is the absorbance of the control reaction and A1 is the absorbance in the presence of CH-EPS. Each sample was analyzed three times.

2.8 | Assessment of Antibacterial Activity

2.8.1 | Microbial Strains and Growth Conditions

The antibacterial activity of CH-EPS was evaluated on six bacterial strains: gram-negative: *Escherichia coli* (ATCC8739), *Pseudomonas aeruginosa* (ATCC 9027), and *Salmonella enterica* (CIP 8039), gram-positive: *Listeria ivanovii* (BUG 496), *Bacillus amyloliquefaciens* (FZB 425), and *Staphylococcus aureus* (ATCC6538). The bacterial strains were incubated on Mueller-Hinton Agar (MHA) at 37°C for 24 h within the Friocell incubator.

2.8.2 | Disk Diffusion Method

The antibacterial activity of CH-EPS was assessed by the disk diffusion method [43]. In brief, 150 µL of culture suspensions containing the tested bacterial strains 10^6 (CFU/mL) were spread evenly on the surface of solid MHA plates. Filter paper disks with a 5 mm diameter were sterilized and then soaked in 10 µL of CH-EPS (0.1 mg per disk). These disks were placed onto inoculated plates and stored at 4°C for 2 h before being incubated at 37°C for 24 h. The antibacterial activity was assessed by measuring the diameter of inhibition zones and comparing them to those of Ampicillin (10 µg per disk), which served as a positive control. The zone inhibition of each size surrounding the tissue was measured using calipers. The antibacterial activity test was conducted in triplicate. The diameter of the inhibition zone was used to assess the degree of bacterial sensitivity to the CH-EPS extract.

2.9 | In Silico Study

In this study, three apoptotic proteins (Bax/Bcl-2 and caspase_3) were used to evaluate the antiapoptotic activity of L-galactose and xylose. The three-dimensional structures of Caspase 3 bound to a covalent inhibitor (PDBid: 3KJF), BCL-2 (PDBid: 6O0K), and the pro-apoptotic protein Bax (PDBid: 1F16) were obtained by downloading them from the RCS PDB from the database at http://www.rcsb.org/pdb. 3D structures of ligands (L-galactose and xylose) were obtained from the PubChem database [44]. Proteins and ligands were prepared prior to the docking process, the water molecules were removed, energy was minimized, and then the site map of Maestro was used for active site prediction. The XP (Extra Precision Mode) docking protocol of Maestro software was employed to carry out the docking process. This method offers a comprehensive investigation, enabling a more in-depth exploration of the molecular interactions that are at play. The optimal docking arrangement was chosen based on the docking pose with the lowest binding free energy between the ligand and receptor. The resulting visual depictions of the docking interactions were observed using Biovia Discovery Studio 2020 (Studio, 2020).

2.10 | Statistical Analysis

The values are represented as the mean ± standard deviation. In order to explore potential correlations between the principal components of CH-EPS and its antioxidant activities the corresponding data were submitted to a normalized principal component analysis (PCA) [45]. Pearson's correlation coefficient was computed to evaluate the significant relationship between the CH-EPS composition and the antioxidant activities. Statistical analyses were conducted using a statistical software program (Xlstat version 19.0).

3 | Results

3.1 | Physicochemical Characterization of CH-EPS

3.1.1 | Yield Extraction and Chemical Compositions of CH-EPS

CH-EPS was extracted from *Halamphora* sp. diatoms using hot water, resulting in an extraction yield of 24.15% of dry weight (DW). The chemical composition of CH-EPS is summarized in Table 1. CH-EPS exhibited a high amount of carbohydrates, reaching 76.33% ± 0.18% of dry weight or total CH-EPS. The protein and lipid contents were low and did not exceed 0.15% ± 0.02% and 0.24% ± 0.006% of CH-EPS, respectively. In addition, sulfate groups and uronic acids contributed 7.56% ± 0.86% and 5.44% ± 0.08%, respectively, to the CH-EPS.

3.2 | Monosaccharide Composition of CH-EPS (GC–MS)

The analysis of monosaccharides showed that the polymers of *Halamphora* sp. are composed of heterogeneous sugars (Table 1). GC–MS analysis showed that CH-EPS displayed

TABLE 1 | Chemical and monosaccharide composition of crude exopolysaccharides (CH-EPS) from *Halamphora* sp.

Composition	Value (% dry weight)
Yield	24.15 ± 1.150
Total carbohydrate	76.33 ± 0.180
Total proteins	0.15 ± 0.026
Total lipids	0.24 ± 0.006
Uronic acid	5.44 ± 0.080
Sulfated groups	7.56 ± 0.860
Neutral sugars (% m/m)	
L-galactose	13.25
Inositol	2.28
Ribitol	9.82
Xylose	40.55
Glucose	9.95
D-galactose	13.00
Mannose	2.90

Values are expressed as mean ± standard deviation ($n = 3$).

a mixed composition of seven monosaccharides, including, L-galactose, inositol, ribitol, xylose, glucose, D-galactose, and mannose. The main component of CH-EPS was xylose (40.55% of monosaccharides), followed by L-galactose (13.25%), and D-galactose (13.00%), with considerable amounts of glucose (9.95%) and ribitol (9.82%). Minor contents of mannose (2.90%) and inositol (2.28%) were also reported.

3.3 | FTIR Analysis of CH-EPS

For a rapid assessment of significant functional groups and polysaccharides binding, the FTIR spectrum of an exopolysaccharides extract from *Halamphora* sp. was obtained, and the results are shown in Figure 1. The FTIR spectrum displays an absorption band at 3430.0 cm^{-1} corresponding to OH groups. Additionally, there are weak bands at 2857.3 and 2924.0 cm^{-1} due to C—H stretching and bending vibrations. The presence of carboxyl groups in CH-EPS is signaled by two characteristic peaks, one at approximately 1629.6 cm^{-1}, corresponding to C—O asymmetric stretching vibration, and another at 1415.2 cm^{-1} related to C—O symmetric stretching vibration. The most significant bands were recorded at 1374.3 and 1350.07 cm^{-1}, which resulted from the stretching vibration of the ester sulfate groups (S═O) (Figure 1). The large band observed at 1152.6 cm^{-1} is attributed to the stretching vibration of C—O in C—O—H bonds and C—O—C glycosidic bond vibration. We assumed that this large band is linked to the presence of the pyranose ring in polysaccharides. Additionally, the minor characteristic absorption at 927.0 cm^{-1} is linked to the C—O—C group present in 3,6-anhydrogalactose, while the bands recorded between 800.0 and 860 cm^{-1} could be attributed to the presence of sulfate groups (Figure 1). Therefore, CH-EPS-FTIR analysis displayed typical uptake peaks (3430.0, 2924.0, 1629.6, 1415.2, 1152.6, and 927.0 cm^{-1}) for algal exopolysaccharides (Figure 1).

3.4 | NMR Analysis of CH-EPS

Figures 2 and 3 show the ^{1}H and ^{13}C NMR spectra of *Halamphora* sp. CH-EPS. The complexity of these spectra reflects the heterogeneity of CH-EPS and confirms the presence of significant exopolysaccharide structures. The spectrum's most informative range is around 5.30–4.35 ppm. The signals at 5.30 and 5.13 ppm were assigned to the anomeric proton of 6-sulfate-α- L- galactopyranose (L-6S) and 3,6-α-L-anhydrogalactose (LA), respectively. However, the signal at 4.36 ppm was caused by the H-1 of β-D-galactose (G') linked to 6-sulfate-α-L-galactopyranose. The signal (at around 4.57 ppm) corresponding to H-1 of β-D-galactose (G) linked to 3,6-α-L-anhydrogalactose was not detected in the ^{1}H NMR spectrum and probably overlapped with the signal of D_2O. Moreover, a series of large and intense signals recorded between

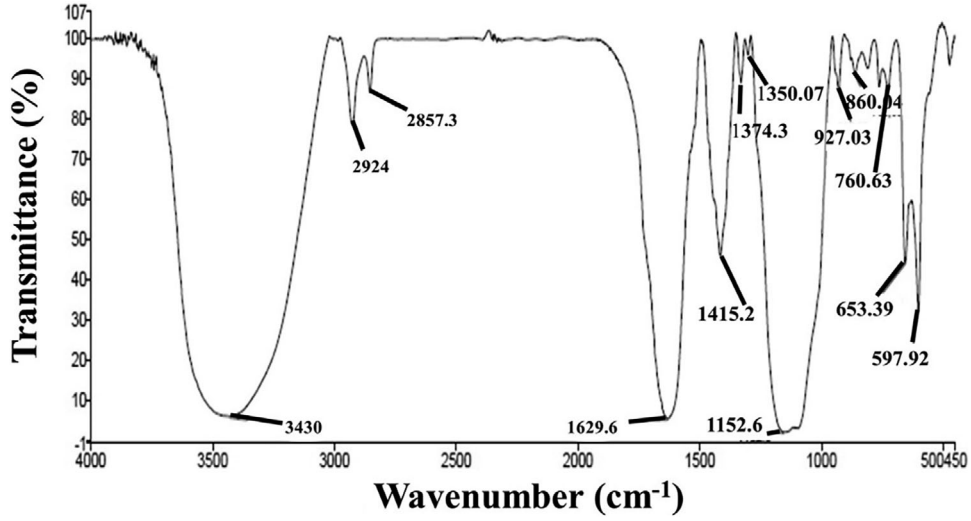

FIGURE 1 | Fourier-transform infrared spectrum (FTIR) spectra of crude exopolysaccharides (CH-EPS) determined according to wavenumber (cm^{-1}) and transmittance (%).

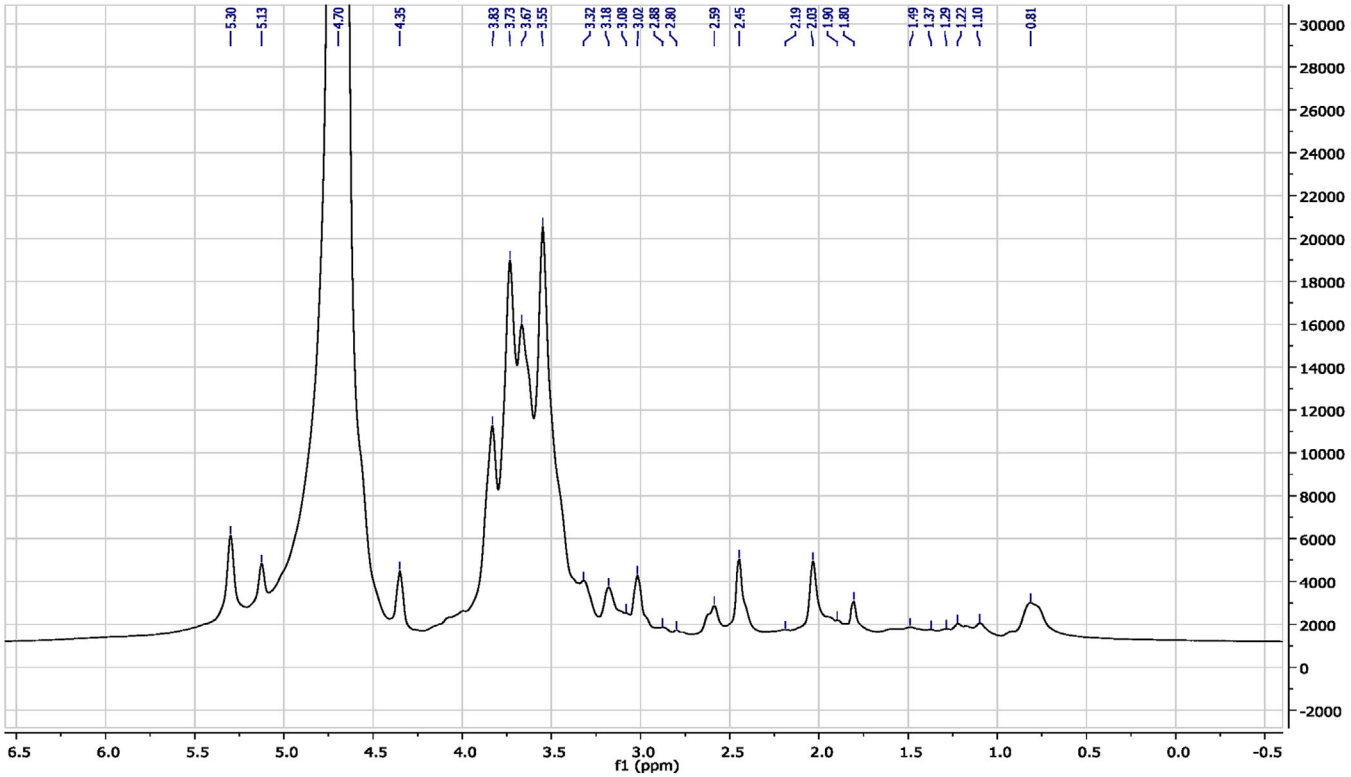

FIGURE 2 | ^{1}H NMR spectrum of *Halamphora* sp. crude exopolysaccharides (CH-EPS).

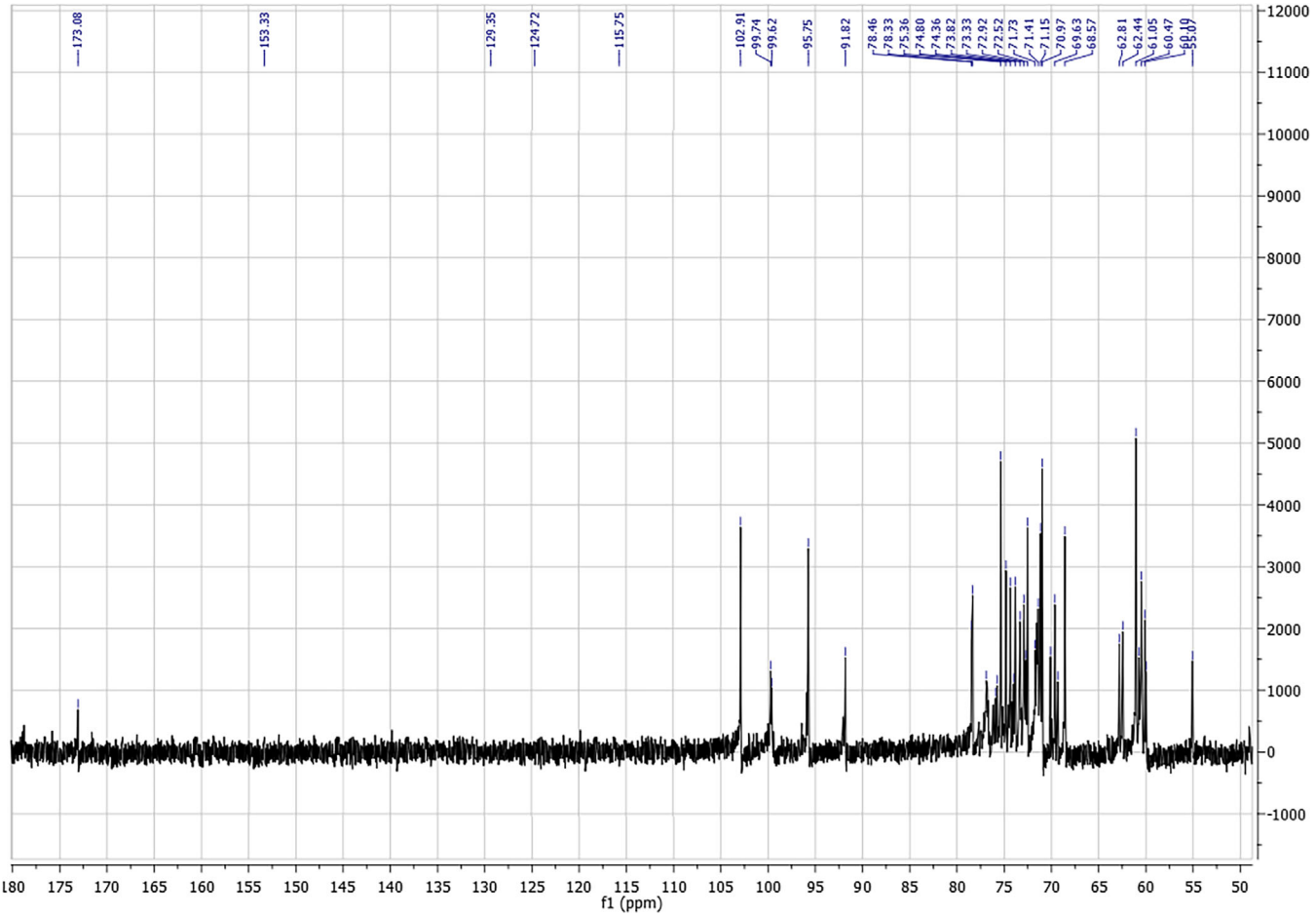

FIGURE 3 | ^{13}C NMR spectrum of *Halamphora* sp. crude exopolysaccharides (CH-EPS).

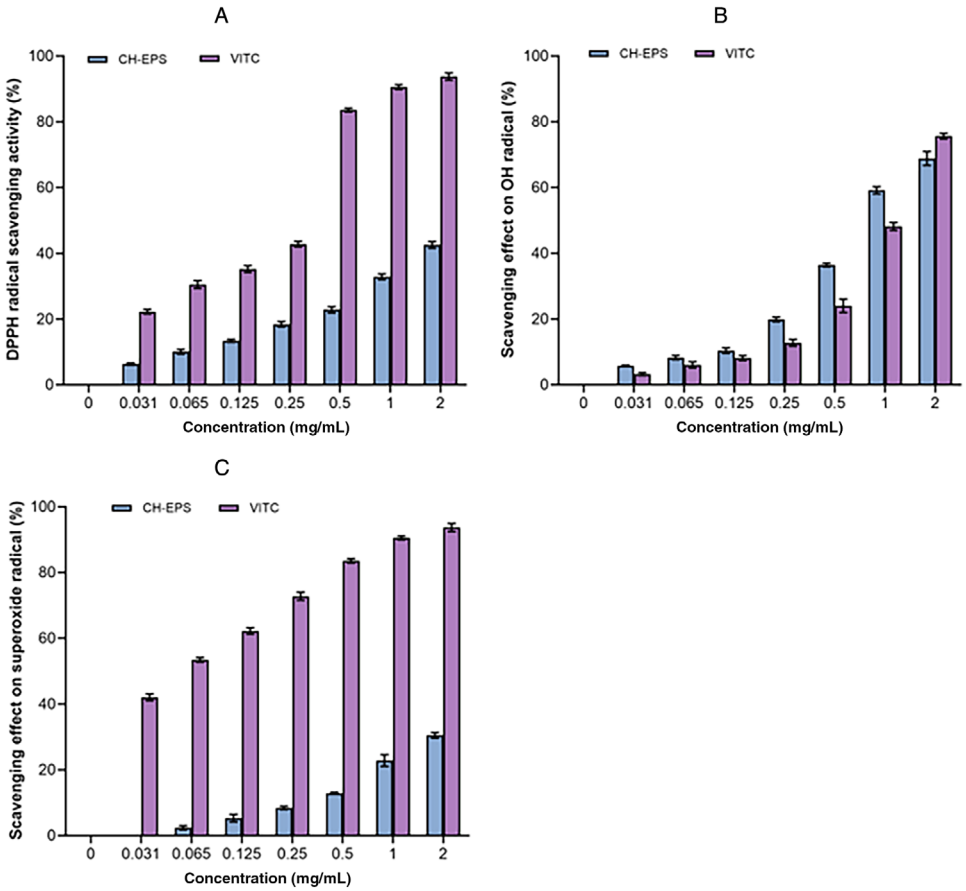

FIGURE 4 | Scavenging effects on (A) 2,2-diphenyl-1-picrylhydrazyl (DPPH), (B) OH, and (C) nitrotetrazolium blue (NBT) assays of Halamphora sp. crude exopolysaccharides (CH-EPS) at different concentrations compared to vitamin C (standard). Values are presented as the mean ± SD of three replicates ($n = 3$).

3.0 and 4.0 ppm were probably linked to the CH_2—O and CH—O groups of the sugars.

In the ^{13}C NMR spectrum, signals from anomeric carbons of the glycoside typically appear in the 90–105 ppm region, while those from non-anomeric carbons are found between 60 and 85 ppm. The anomeric region of CH-EPS (δ 99–105) exhibits three prominent signals (Figure 3), which were attributed to C-1 of β-D-galactose (G') linked to 6-sulfate-α-L-galactopyranose at 102.9 ppm; C-1 of 6-sulfate-α-L-galactopyranose unit at 99.7 ppm and C-1 of 3,6-α-L-anhydrogalactose at 99.6 ppm. The signal corresponding to C-1 of β-D-galactose (G) bound to 3,6-α-L-anhydrogalactose was not detected in the ^{13}C NMR spectrum and probably overlapped with the signal at 102.9 ppm. This spectrum showed, among others, four CH_2 signals at 69.6, 68.5, 62.4, and 61.0 ppm attributed to C-6 of 3,6-α-L-anhydrogalactose, 6-sulfate-α-L-galactopyranose (L-6S), β-D-galactoses (G), and (G′) residues, respectively. Also, the spectrum displayed two specific signals at δ 55.0 and 173.0 ppm revealing the presence of O-methyl sugar residue and carboxyl groups, respectively, in the CH-EPS.

3.5 | Antioxidant Activities of CH-EPS

The total antioxidant capacity (TAC) of CH-EPS exhibited a high value of 8.63 ± 0.36 mg vitamin C equivalent/g of sample.

3.5.1 | Scavenging Effects of CH-EPS on DPPH Radicals

The DPPH test was used to determine the antioxidant activity of CH-EPS. The results for various concentrations (Figure 4A) indicated that CH-EPS exhibited moderate free radical scavenging activity, but it was significantly lower than that of vitamin C ($p < 0.05$). Indeed, the highest scavenging activity was recorded at 2 mg/mL of CH-EPS corresponding to a low DPPH absorbance which did not exceed 42.52 ± 1.37%.

3.5.2 | Hydroxyl Radical Scavenging Effects of CH-EPS

Figure 4B displays the hydroxyl radical scavenging ability of CH-EPS. CH-EPS exhibited a high reduction in hydroxyl radicals with the concentration-dependent pattern. The maximum inhibition reached 68.82 ± 1.37% at 2 mg CH-EPS/mL corresponding to an IC_{50} value of 0.84 mg/mL. However, the IC_{50} of vitamin C was 1.32 mg/mL.

3.5.3 | Scavenging Effect of CH-EPS on Superoxide Radical

As shown in Figure 4C, CH-EPS was a poor scavenger of superoxide radicals compared to vitamin C ($p < 0.05$).

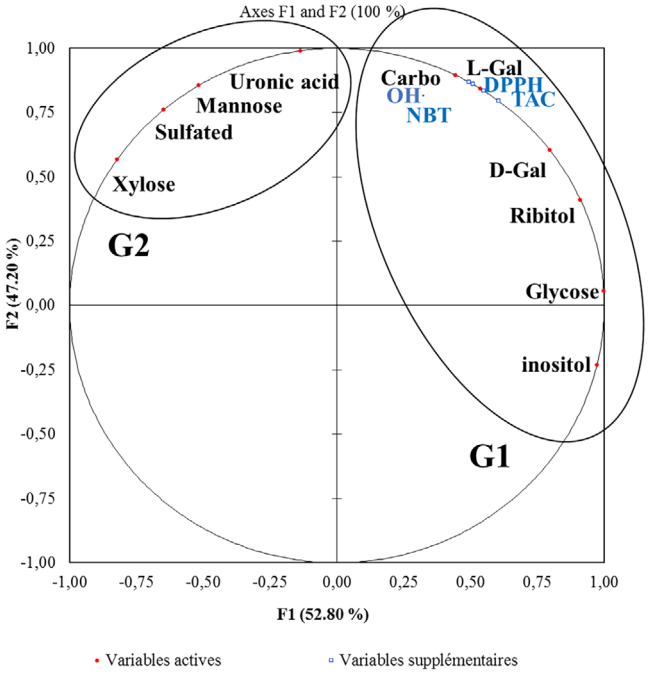

FIGURE 5 | Principal component analysis (PCA) of the monosaccharide component crude exopolysaccharides (CH-EPS) from *Halamphora* sp. and antioxidant capacity.

While the sulfate content on the CH-EPS was high (7.56% of DW, Table 1), the maximum braking value did not exceed 30.52% ± 3.37.

3.6 | Relationship Between Antioxidant Activity and Principal Components of CH-EPS

The principal component analysis (PCA) displays potential correlations between the principal components of CH-EPS and its antioxidant activity (Figure 5). Axes F1 and F2 accounted for 100% of the total variance and displayed two distinct groups. Axis F1 selected positively the first group (G1), which was composed of D-galactose, ribitol, glucose, and inositol. However, F1 selected negatively the monosaccharide xylose. F2 axis selected the group (G2) composed of total carbohydrate, L-galactose, mannose, xylose, uronic acid, and sulfated compounds, which are coupled to DPPH, TAC, NBT, and OH·. Pearson correlation revealed a strong correlation between the levels of L-galactose, and NBT (r = 1; $p < 0.01$), OH (r = 0.99; $p < 0.05$), and DPPH (r = 0.99; $p < 0.05$) (Table 2). Moreover, D-galactose and ribitol were correlated positively with TAC, NBT, DPPH, and OH.

3.7 | Antibacterial Assay

The antibacterial activity of *Halamphora* sp. CH-EPS was tested against six bacterial strains, and its effectiveness was determined through qualitative and quantitative assessment of inhibition zone diameters (IZD) (Table 3). Results show that CH-EPS inhibited the growth of nearly all tested bacterial strains. EPS extract shows a low activity against Gram (+) bacteria, producing zones of inhibition 10–12 mm in diameter compared to that of ampicillin (IZD = 14–25 mm) (Table 3). However, for Gram (−) bacteria, a moderate potential antimicrobial activity of 8 mm was observed against *E. coli* (ATCC 8739), while it was weaker against *Pseudomonas aeruginosa* (ATCC 9027) and *Salmonella enterica* (CIP 8039) about 7 and 7.6 mm, respectively.

3.8 | Antiapoptotic Effect: In Silico Study

A molecular docking study of the activity of L-galactose and xylose against apoptotic proteins revealed that the best docking score was generated due to the interaction of xylose and caspase_3, which was −6.9 kcal/mol, as shown in Table 4. L-galactose generated a docking score of −5 kcal/mol with caspase_3, BCL-2, and Bax (Table 4). Different hydrogen bonds were generated due to the interaction of the ligands and apoptotic proteins. Ten hydrogen bonds were shown from the interaction of caspase_3 and L-galactose: ARG 64A, (2), HIS 121A (2), GLN 161A, CYS163A (2), SER205B, and ARG207B (2). The bonds occurred at a very small distance between 1.8 and 2.8 Å (Table 5). The interaction of caspase_3 and xylose generated 5 hydrogen bonds with residues ARG207B, ASN208B, TRP 214B, and PHE250B (2) (Arg207, Arg64, Ser205) (Figure 6). As shown in Table 6, the Bax protein and L-galactose interacted with 14 H-bonds, which resulted in a docking score of −5.8 kcal/mol, while the interaction of Bax and xylose resulted in 6 H-bonds and a docking score of −4.5 kcal/mol (Figure 7). BCL-2 showed the least number of H-bonds with both L-galactose and xylose, and two (TYR108A and ARG146A) and three (ASP 103A and ARG107A) H-bonds were generated, respectively (Figure 8).

4 | Discussion

CH-EPS was extracted from *Halamphora* sp. diatoms using hot water; the extraction yield was 24.15% of dry weight (DW), which is similar to that of *Cylindrotheca closterium* (23%) [46]. The soluble sulfated polysaccharides of the diatoms *Chaetoceros affinis* and *Chaetoceros debili* ranged between 16 and 40 mg/L [47]. The differences in the strains, culture conditions, extraction methods, and growth phase of the culture make it difficult to compare the results with those in the literature. The biosynthesis of polysaccharides is linked to the ability of microalgae to grow under unfavorable conditions [48, 49] The environmental (e.g., salinity, nutrient limitation, temperature, growth phase, etc.) and nutritional factors (e.g., Mg^{2+}, K^{+}, Ca^{2+}, etc.) inherent in microalgae technology can affect the synthesis of polysaccharides [50]. Thus, optimizing process conditions and culture infrastructure for microalgae boosts cell growth rate, biomass production, and polysaccharides yield [49]. Benthic diatoms produce the highest concentration of EPS when cultured under nutrient-restricted conditions [51–53]. Components of the diatom carbohydrate pool may therefore fall into different extracts [53–55]. Carbohydrate composition, size, and structural form influence the degree to which EPS bind to sediments, respond to dehydration, and are degraded by bacteria [21, 56] These characteristics are crucial to the significant roles that EPS play in marine sediments, where they act as agents for biostabilization [54] and contributing to carbon pump in the environment [53, 57] Our results showed that CH-EPS exhibited a high amount of carbohydrates, reaching 76.33 ± 0.18% of dry weight or total CH-EPS. The protein and

TABLE 2 | Correlation matrix (Pearson–Bravais) between the different compounds of crude exopolysaccharides (CH-EPS) and the antioxidant activities.

Variables	Carbo	Uronic acid	Sulfated	Xylose	D-Gala	Glycose	Ribitol	Mannose	Inositol	L-Gala	TAC	DPPH	OH	NBT
Carbo	1													
Uronic acid	0.827**	1												
Sulfated	0.394*	0.842**	1											
Xylose	0.143	0.674**	0.966**	1										
D-Gala	0.895**	0.490*	−0.057	−0.313	1									
Glycose	0.494*	−0.079	−0.604	−0.790	0.830**	1								
Ribitol	0.773**	0.283*	−0.279	−0.518	0.975**	0.934**	1							
Mannose	0.538*	0.918**	0.987**	0.911**	0.105	−0.467	−0.120	1						
Inositol	0.224*	−0.363	−0.808	−0.933	0.635**	0.958**	0.791**	−0.702	1					
L-Gala	0.994**	0.762**	0.292*	0.035	0.938**	0.585*	0.837**	0.444*	0.327*	1				
TAC	0.982**	0.706**	0.213*	−0.047	0.963**	0.650**	0.879**	0.368*	0.404*	0.997**	1			
DPPH	0.997**	0.783**	0.324*	0.069	0.926**	0.558*	0 ;818**	0.473*	0.295*	0.999**	0.993**	1		
OH·	0.998**	0.794**	0.341*	0.086	0.919**	0.543*	0.808**	0.489*	0.279*	0.999**	0.991**	1.000**	1	
NBT	0.992**	0.752**	0.278*	0.020	0.943**	0.598*	0.845**	0.430*	0.342*	1.000**	0.998**	0.999**	0.998**	1

Values are the mean of triplicate determination.

*$p < 0.05$.

**$p < 0.01$.

Abbreviations: Carbo: carbohydrate, D-Gala: D-galactose, DPPH: 2,2-diphenyl-1-picrylhydrazyl, L-Gala: L-galactose, NBT: nitrotetrazolium blue, OH: hydroxyl, TAC: total antioxidant capacity.

TABLE 3 | Antibacterial activity of *Halamphora* sp. crude exopolysaccharides (CH-EPS).

		Inhibition zone diameter (mm)	
	Bacteria strains	**CH-EPS**	**Ampicillin**
Gram+	*Listeria ivanovii* (BUG 496)	10 ± 0.4	25 ± 0.1
	Bacillus amyloliquefaciens (FZB 425)	12 ± 0.4	19 ± 0.2
	Staphylococcus aureus (ATCC 6538)	11 ± 0.2	20 ± 0.3
Gram−	*Pseudomonas aeruginosa* (ATCC 9027)	7.6 ± 0.3	22 ± 0.4
	Escherichia coli (ATCC 8739)	8 ± 0.1	25 ± 0.2
	Salmonella enterica (CIP 8039)	7 ± 0.3	14 ± 0.2

Values are mean ± SD of triplicate determination. According to CLSI (2020), all bacteria strains are resistant to CH-EPS.

TABLE 4 | Docking scores of the interaction of apoptotic proteins with L-galactose and xylose.

		Docking score (kcal/mol)		
Ligand	**PubChem ID**	**Caspase_3**	**BCL-2**	**Bax**
L-galactose	84996	−5.85	−5.56	−5.8
Xylose	135191	−6.9	−4.50	−4.5

lipid contents were low and did not exceed 0.15 ± 0.02% and 0.24 ± 0.006 of CH-EPS, respectively. The protein content of the EPS isolated from various planktonic diatoms ranged from 0% to 30% [18]. The lowest protein content in CH-EPS can be due to the hot water extraction method leading to the denaturation of almost all proteins. Our results corroborate several studies that stated that carbohydrates are the main components of EPS and that proteins are a minor fraction in the diatoms *Cylindrotheca closterium*, *Navicula salinarum*, and *Amphora* [52, 53]. According to the literature, the lipid content of polysaccharides extracted from microalgae is generally below 4% and it depends on several factors, such as climate, stage development of cells, and their geographic location [49, 58]. We assumed that EPS extracted from *Halamphora* sp. was highly pure. In addition, sulfate groups and uronic acids contributed to 7.56 ± 0.86% and 5.44 ± 0.08% of the CH-EPS, respectively. EPS polymers synthesized under extreme environmental conditions tended to exhibit higher complexity, characterized by increased uronic acid and sulfate content. [16] The uronic acids have been recorded in diatoms *Cylindrotheca*

TABLE 5 | Protein residues generated H-bonds of the interaction between caspase 3 and ligands.

Complex	Index	Residue	AA	Distance H–A	Distance D–A	Donor angle	Donor atom	Acceptor atom
Caspase_3 and L-galactose	1	64A	ARG	2.38	3.3	154.71	458 [Ng+]	3872 [O2]
	2	64A	ARG	1.94	2.89	154.1	461 [Ng+]	3872 [O2]
	3	121A	HIS	2.12	3.01	152.06	3867 [O3]	1409 [Nar]
	4	121A	HIS	2.77	3.7	163.1	3870 [O3]	1409 [Nar]
	5	161A	GLN	2.22	3.2	160.29	2052 [Nam]	3872 [O2]
	6	163A	CYS	2.85	3.59	130.87	2071 [Nam]	3868 [O3]
	7	163A	CYS	2.68	3.46	137.76	3868 [O3]	2076 [S3]
	8	205B	SER	2.06	2.97	156.89	3869 [O3]	2650 [O2]
	9	207B	ARG	2.16	3.08	147.86	2689 [Ng+]	3872 [O2]
	10	207B	ARG	1.81	2.82	170.04	2692 [Ng+]	3870 [O3]
Caspase_3 and xylose	1	207B	ARG	2.04	2.9	150.97	3868 [O3]	2685 [O2]
	2	208B	ASN	2.72	3.58	143.14	2713 [Nam]	3871 [O3]
	3	214B	TRP	2.1	3.05	157.4	2791 [Nar]	3871 [O3]
	4	250B	PHE	2.17	3.04	143.75	3395 [Nam]	3870 [O3]
	5	250B	PHE	1.86	2.65	139.96	3870 [O3]	3398 [O2]

Abbreviations: AA: amino acids, ARG: arginine, ASN: asparagine, CYS: cysteine, GLN: glutamine, HIS: histidine, PHE: phenylalanine, SER: serine, TRP: tryptophan.

TABLE 6 | Protein residues generated H-bonds of the interaction of Bax and ligands.

	Index	Residue	AA	Distance H–A	Distance D–A	Donor angle	Donor atom	Acceptor atom
Bax and L-galactose	1	32A	GLN	2	2.95	166.1	9146 [O3]	734 [O3]
	2	34A	ASP	3.11	3.88	137.92	777 [O3]	9148 [O2]
	3	36A	SER	2.25	3.13	145.41	853 [N3+]	9146 [O3]
	4	37A	TYR	0.58	1.52	160.89	9143 [O3]	871 [N3]
	5	38A	LYS	2.89	3.51	119.83	916 [N3]	9143 [O3]
	6	39A	GLY	2.21	3.17	158.89	956 [N3]	9144 [O3]
	7	45A	LEU	2.89	3.86	176.99	9145 [O3]	1126 [O2]
	8	103A	ASP	1.69	2.66	176	9135 [O3]	3187 [O.Co2]
	9	107A	ARG	2.92	3.53	119.18	3385 [Ng+]	9135 [O3]
	10	119A	LYS	2.94	3.57	121.18	4023 [N3+]	9134 [O3]
	11	176A	TRP	2.85	3.2	102.28	6695 [O3]	9147 [O3]
	12	180A	TYR	1.85	2.75	152.63	9147 [O3]	6841 [N1]
	13	184A	HIS	3.08	3.98	147.77	7012 [N3]	9143 [O3]
	14	277B	HIS	3.21	4.09	147.32	9108 [Npl]	9147 [O3]
Bax and xylose	1	32A	GLN	2.09	2.9	141.05	2803 [O3]	269 [O2]
	2	32A	GLN	1.94	2.86	160.2	2804 [O3]	269 [O2]
	3	39A	GLY	3.46	4.08	123.59	2806 [O3]	376 [O2]
	4	39A	GLY	2.93	3.41	109.94	373 [Nam]	2804 [O3]
	5	44A	GLU	1.78	2.75	169.16	2805 [O3]	434 [O.Co2]
	6	45A	LEU	2.91	3.84	152.33	441 [Nam]	2802 [O3]

Abbreviations: AA: amino acids, ARG: arginine, ASP: aspartic acid, GLN: glutamine, GLU: glutamic acid, GLY: glycine, HIS: histidine, LEU: leucine, LYS: lysine, SER: serine, TRP: tryptophan, TYR: tyrosine.

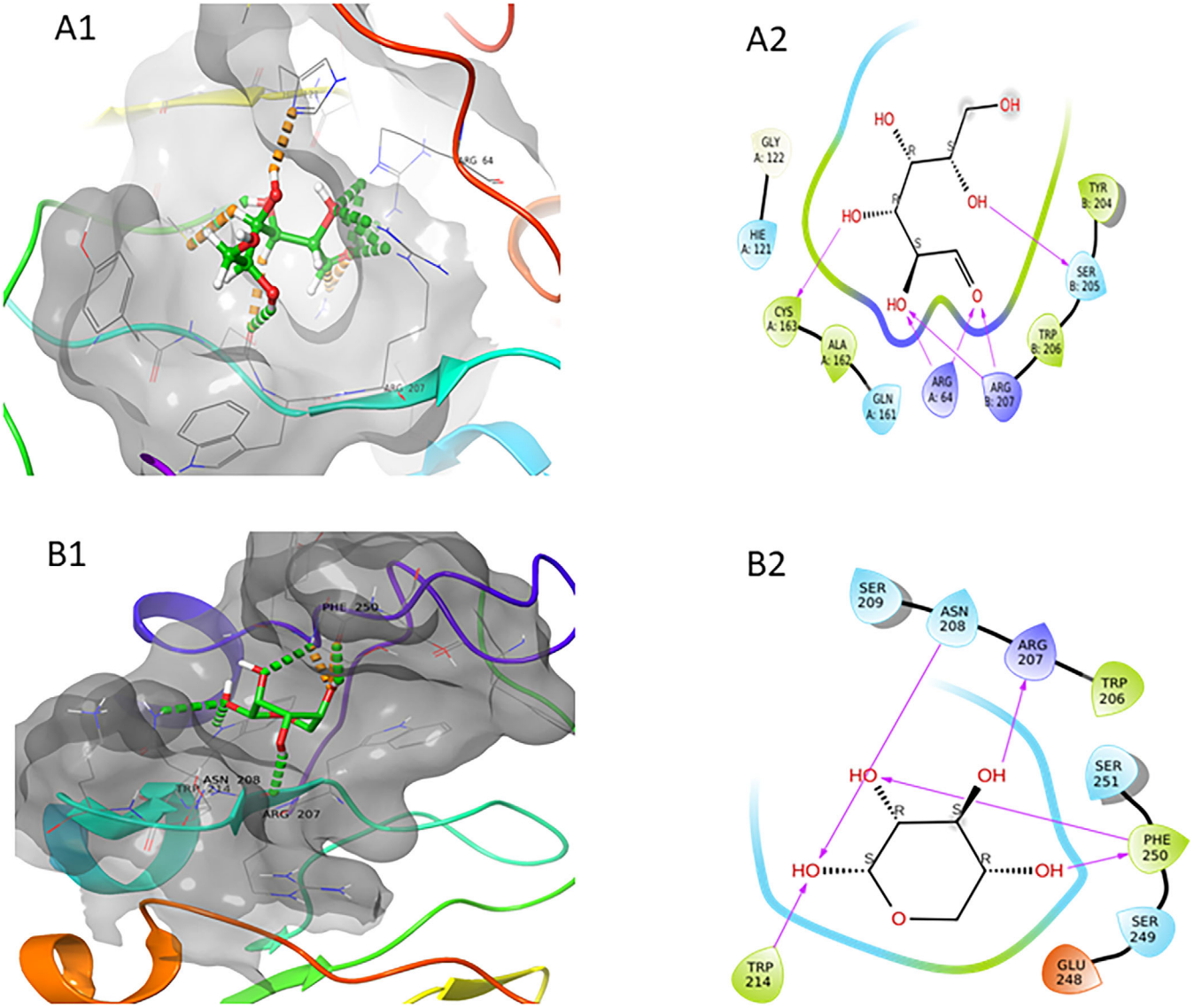

FIGURE 6 | 3D and 2D molecular docking of the Caspase 3 ligands. A1 and B1 represent the 3D structures of protein (gray) and ligands (L-galactose and xylose, respectively) in green, white, and red colors in the center, and the dashed green line represents the hydrogen bond. A2 and B2 represent the 2D interaction protein residues and ligands (L-galactose and xylose, respectively) in black, and hydrogen bonds are indicated by purple arrows.

closterium, *Navicula salinarum, N. subinflata*, *Craspedosauros australis*, and *Pinnularia viridis* reporting that the uronic acids and sulfated groups can confer free radical scavenging abilities [52, 55, 59–61].

Our GC–MS findings were similar to the monosaccharide composition of EPS from other diatoms [14]. The composition of EPS monosaccharides can change significantly depending on the extraction method, strains, species, and growth conditions [62]. The composition of CH-EPS in monosaccharides partially falls on the list of standard diatom monosaccharides [14]. EPS from diatoms has two main compositional characteristics: (1) they are composed of heteropolysaccharides, which may be sulfated [63], and (2) they contain rhamnose, fucose, galactose, glucose, mannose, xylose, and/or uronic acids and arabinose in smaller amounts [25].

The FTIR spectrum displays a broad absorption peak at 3430.0 cm^{-1} characteristic of OH groups and weak bands at 2924.0 and 2857.3 cm^{-1}, which have been attributed to CH stretches [64]. C═O symmetric stretches were verified by a high peak at 1629.6 cm^{-1} [65]. The 1415.2 cm^{-1} peak represented the characteristic absorbance of C─H bands, while the 1152.6 cm^{-1} power band suggested that the characteristic sugar fractions had a pyranose configuration [25]. The significant peaks were recorded at 1374.3 and 1350.07 cm^{-1}, corresponding to the bending and stretching vibrations of ester sulfate groups (S═O) [62, 63].

Furthermore, the slight characteristic absorptions at 800.0–927.0 cm^{-1} may indicate the presence of α-linked and β-linked glycosyl groups in the main chain [66]. NMR spectroscopy is a nondestructive analysis that provides important information for the structural characterization of algal polysaccharides [64]. ^{13}C NMR shows that our polysaccharide CH-EPS is a sulfated type of exopolysaccharide (α-L-galactose-6-sulfate at δ 102.9). The ^{1}H and ^{13}C NMR data support the findings of chromatography analysis, indicating the existence of specific monosaccharides, including

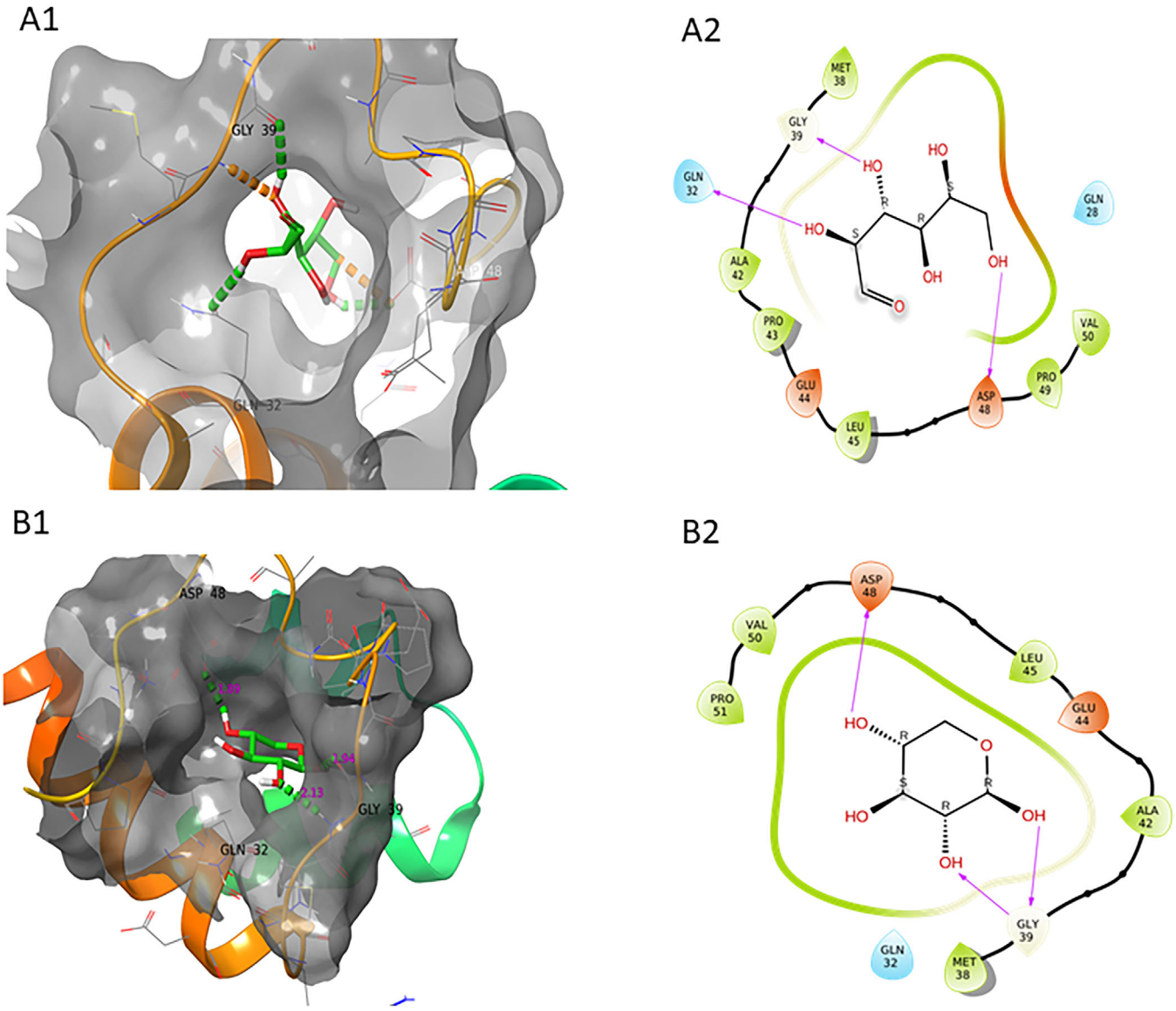

FIGURE 7 | 3D and 2D molecular docking of Bax and ligands. A1 and B1 represent the 3D structures of protein (gray) and ligands (L-galactose and xylose, respectively) in green, white, and red colors in the center, and the dashed green line represents the hydrogen bond. A2 and B2 represent the 2D interaction protein residues and ligands (L-galactose and xylose, respectively) in black, and hydrogen bonds are indicated by purple arrows.

glucose and β-D-galactose. The anomeric region of ^{13}C NMR (δ 99–105) exhibits three principal signals, assigned from the literature data as C-1 of β-D-galactose linked to α-L-galactose-6-sulfate at δ 102.9; C-1 of α-L-galactose-6-sulfate unit at δ 99.7 and C-1 of 3,6-α-L-anhydrogalactose at δ 99.6 [63, 67] Due to the complexity of the polysaccharides structure, only certain structural groups were identified using FTIR and ^{13}C NMR spectroscopy. Further study using two-dimensional NMR is required to determine the accurate and detailed structure of CH-EPS.

Our results show that CH-EPS had a high antioxidant activity (TAC) as a reducing agent because several authors reported that 9.2 mg vitamin C equivalent/g of sample (close to our TAC value of 8.63 mg vitamin C equivalent/g of sample) corresponds to a high antioxidant activity [68]. The results for various concentrations showed that CH-EPS had a moderate DPPH free radical scavenging activity of about 42.52 ± 1.37%, lower than that of Vitamin C. In a previous study, an aqueous extract of extracellular polysaccharides from *Chlorella vulgaris* demonstrated an activity reaching 100% radical inclusion in the DPPH test [69]. Our data revealed a difference in the results, which can be largely attributed to the chemical composition of the extract for each EPS. In fact, the aqueous extract of *Chlorella vulgaris* EPS was rich in phenolic compounds, whereas that of *Halamphora* sp. was abundant in sulfated carbohydrates.

Hydroxyl radicals can be a product of the immune response and are therefore short-lived. These free radicals are highly reactive and can easily penetrate the cell membrane at certain sites, react with most biological macromolecules, such as carbohydrates, nucleic acids, lipids, and amino acids, and cause harm to human health. Therefore, it is crucial to remove excess hydroxyl radicals [70]. This suggests that CH-EPS could be considered a strong inhibitor of OH$^{\cdot}$ radicals. This activity may be due to the sulfate and uronic acid content, as reported by previous studies [71, 72]. However, our CH-EPS is a poor scavenger of superoxide radicals

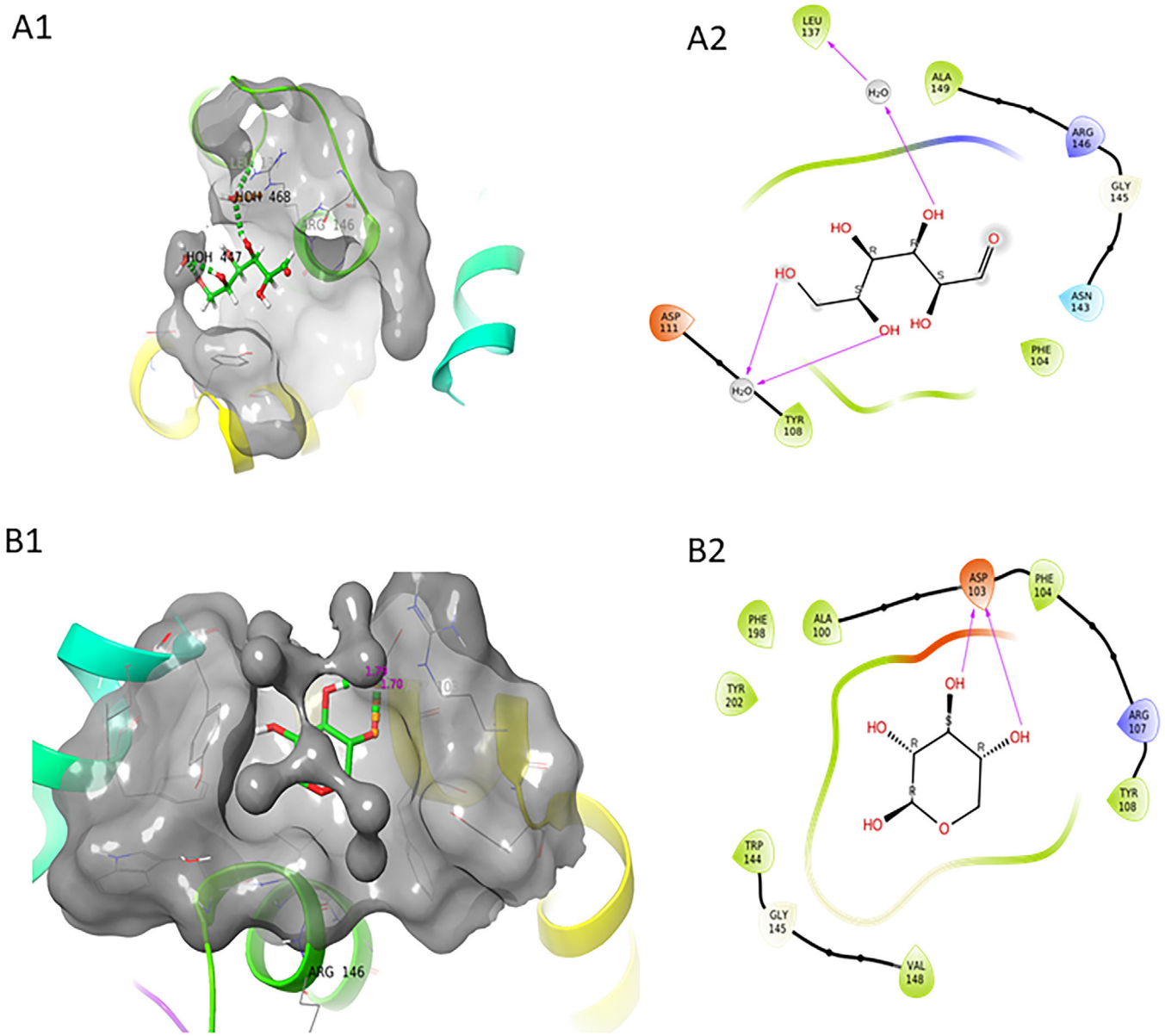

FIGURE 8 | 3D and 2D molecular docking of Bcl-2 and ligands. A1 and B1 represent the 3D structures of protein (gray) and ligands (L-galactose and xylose, respectively) in green, white, and red in the center, and the dashed green line represents the hydrogen bond. A2 and B2 represent the 2D interaction protein residues and ligands (L-galactose and xylose, respectively) in black, and hydrogen bonds are indicated by purple arrows.

compared to that of vitamin C. Numerous studies have shown that the ability to scavenge superoxide radicals depends on the sulfate content [71, 73]. While the sulfate content on the CH-EPS was high (7.56% of DW, Table 1), the maximum braking value did not exceed 30.52% ± 3.37%. Costa et al. [74] suggested that the scavenging ability of superoxide anions depends more on the spatial arrangement of the sulfated groups than on the sulfate content. Among the polysaccharides of microalgae, EPS has become interesting due to its bioactive properties. Acidic compounds, along with sulfate and carboxyl groups, contribute to the anionic character of polysaccharides, which in turn influences their diverse biological activities [75]. The antioxidant, anti-inflammatory, anticancer, and antimicrobial properties of polysaccharides contribute to their use in several fields. Particularly, the monosaccharides arabinose, rhamnose, and galactose which are associated with antioxidant activities [49, 76] In our study, the highest TAC of CH-EPS was attributed mainly to the scavenging effects on hydroxyl radicals, probably due to the uronic acid, sulfated group, L and D-galactose, and xylose content.

Researchers are actively seeking natural antimicrobial agents as alternatives for combating infectious illnesses. Recent studies conducted on various marine microorganisms have demonstrated their antibacterial properties, attributed to the presence of diverse bioactive components [77, 78]. This study revealed that CH-EPS displayed inhibitory effects on the growth of several bacterial strains. Indeed, the crude extract showed moderate activity against Gram-positive bacteria such as *Listeria ivanovii* (BUG 496), *Bacillus amyloliquefaciens* (FZB 425), and *Staphylococcus aureus* (ATCC6538). However, the antimicrobial activity of CH-EPS exhibited a weaker activity against Gram (–) bacteria such *as Pseudomonas aeruginosa* (ATCC 9027) and *Salmonella enterica*

(CIP 8039), with zones of 7 and 7.6 mm, respectively. Our findings corroborate with those of Mashjoor et al. [79], who reported that Gram-positive bacteria are more sensitive to marine polysaccharide extracts than Gram-negative bacteria. The observed greater effect of *Halamphora* sp. on Gram-positive bacteria may be due to the absence of an outer phospholipid membrane. This latter present in Gram-negative bacteria, limits the diffusion of hydrophobic compounds through their lipopolysaccharides envelope, leading to the leakage of essential intracellular components and the alteration of bacterial enzyme systems [80]. Our study provides additional molecular-level insights into the roles of CH-EPS in *Halamphora* sp., particularly highlighting their functions as reactive oxygen species chelators and antibacterial agents.

According to molecular docking studies, xylose exhibits the best docking score with caspase 3, which could be used as a possible inhibitor. This finding is supported by the presence of a high number of strong hydrogen and hydrophobic bonds. As a result of the interaction of xylose and caspase 3, the interaction blocked the conserved and essential residues of the active site of caspase 3 (Arg207, Arg64, and Ser205) [81]. Similarly, xylose blocked some of these essential residues. Additionally, L-galactose showed a favorable docking score with caspase 3 and Bax protein. The key residue (ASP 103) of Bcl-2 [82] is blocked by two strong hydrogen bonds as a result of the interaction of xylose, which could result in the loss of the activity of this protein.

5 | Conclusions

The present study was performed to partially characterize the crude aqueous extracellular polysaccharides of Tunisian diatom *Halamphora* sp. SB1MK575516.1 and to investigate its antioxidant, antibacterial antiapoptotic properties. The results obtained by FTIR, GC–MS, and NMR analyses showed that CH-EPS was an extracellular polysaccharide composed of xylose, L-galactose, D-galactose, glucose, ribitol, mannose, and inositol. The CH-EPS extracted from *Halamphora* sp. demonstrated high in vitro values for total antioxidant capacity and hydroxyl radical scavenging activity. These high antioxidant properties were probably due to the high content of exopolysaccharides extract, L and D galactose, ribitol, and uronic acid. In addition, CH-EPS showed moderate antibacterial activity, especially on Gram-positive strains. The binding affinity with pro-apoptotic proteins such as caspase 3 showed the antiapoptotic capacity of this crude aqueous extracellular polysaccharides of Tunisian brown microalga in *Halamphora* sp. Our results strongly suggest that CH-EPS has the potential to be a promising new agent with antioxidant, antibacterial, and antiapoptotic properties. However, further research is needed to refine extraction and purification methods and to thoroughly evaluate its biological functions.

Author Contributions

Data collection: F. Ben Mansour and W. Guermazi; Design of the study: W. Guermazi and H. Ayadi; Investigation and data analysis: F. Ben Mansour, W. Guermazi, M. Chamkha, K. Bellassoued, H. Ben Salah, and W. Aldahmash; Drafting the manuscript: F. Ben Mansour, W. Guermazi, and A. H. Harrath; Critical revision of the manuscript: W. Guermazi, A. H. Harrath, and H. Ayadi

Acknowledgements

The authors acknowledge the "Ministry of Higher Education, Scientific Research and Technology, Tunisia", for the support of this study. The authors also extend their appreciation to Researchers Supporting Project number RSP2024R17, King Saud University, Riyadh, Saudi Arabia.

Ethics Statement

The authors have nothing to report.

Conflicts of Interest

The authors declare no conflicts of interest.

Data Availability Statement

All necessary data generated or analyzed during this study are presented in this article and additional data could be available from the corresponding author upon request.

References

1. M. Chen, Y. Zhou, J. Huang, P. Zhu, X. Peng, and Y. Wang, "Liposome-Based Delivery Systems in Plant Polysaccharides," *Journal of Nanomaterials* 2012 (2012): 50.

2. R. P. Da Silva, T. A. Rocha-Santos, and A. C. Duarte, "Supercritical Fluid Extraction of Bioactive Compounds," *Trac Trends in Analytical Chemistry* 76 (2016): 40–51.

3. S. Sergeant, E. Rahbar, and F. H. Chilton, "Gamma-Linolenic Acid, Dihommo-Gamma Linolenic, Eicosanoids and Inflammatory Processes," *European Journal of Pharmacology* 785 (2016): 77–86.

4. T. A. Conde, B. F. Neves, D. Couto, et al., "Microalgae as Sustainable Bio-Factories of Healthy Lipids: Evaluating Fatty Acid Content and Antioxidant Activity," *Marine Drugs* 19 (2021): 357.

5. V. Castro, R. Oliveira, and A. C. Dias, "Microalgae And Cyanobacteria as Sources of Bioactive Compounds for Cosmetic Applications: A Systematic Review," *Algal Research* 76 (2023): 103287.

6. B. F. Lucas and T. A. Brunner, "Attitudes and Perceptions Towards Microalgae as an Alternative Food: A Consumer Segmentation in Switzerland," *Algal Research* 78 (2024): 103386.

7. S. Boukhris, K. Athmouni, I. Hamza-Mnif, et al., "The Potential of a Brown Microalga Cultivated in High Salt Medium for the Production of High-Value Compounds," *BioMed Research International* 2017 (2017): 4018562.

8. I. Dahmen-Ben Moussa, D. Belhaj, and H. Ayadi, "Optimization of Extraction Process of Polyphenols From Wild Halotolerant Cyanobacteria, Phormidium Versicolor (NCC 466)," *Biomass Conversion and Biorefinery* 14 (2022): 1–11.

9. T. Belghith, K. Athmouni, J. Elloumi, W. Guermazi, T. Stoeck, and H. Ayadi, "Biochemical Biomarkers in the Halophilic Nanophytoplankton: Dunaliella Salina Isolated From the Saline of Sfax (Tunisia)," *Arabian Journal for Science and Engineering* 41 (2016): 17–24.

10. W. Guermazi, S. Masmoudi, N. A. Trabelsi, et al., "Physiological and Biochemical Responses in Microalgae Dunaliella Salina, Cylindrotheca closterium and Phormidium Versicolor NCC466 Exposed to High Salinity and Irradiation," *Life* 13 (2023): 313.

11. S. Gammoudi, K. Athmouni, A. Nasri, et al., "Optimization, Isolation, Characterization and Hepatoprotective Effect of a Novel Pigment-Protein Complex (Phycocyanin) Producing Microalga: Phormidium Versicolorncc-466 Using Response Surface Methodology," *International Journal of Biological Macromolecules* 137 (2019): 647–656.

12. C. Balavigneswaran, T. S. J. Kumar, R. M. Packiaraj, A. Veeraraj, and S. Prakash, "Anti-Oxidant Activity of Polysaccharides Extracted From Isocrysis Galbana Using Rsm Optimized Conditions," *International Journal of Biological Macromolecules* 60 (2013): 100–108.

13. D. Belhaj, D. Frikha, K. Athmouni, et al., "Box-Behnken Design for Extraction Optimization of Crude Polysaccharides From Tunisian Phormidium Versicolor Cyanobacteria (Ncc 466): Partial Characterization, in Vitro Antioxidant and Antimicrobial Activities," *International Journal of Biological Macromolecules* 105 (2017): 1501–1510.

14. S. M. Myklestad, "Release of Extracellular Products by Phytoplankton With Special Emphasis on Polysaccharides," *Science of the Total Environment* 165 (1995): 155–164.

15. A. Chiovitti, A. Bacic, J. Burke, and R. Wetherbee, "Heterogeneous Xylose-Rich Glycans are Associated With Extracellular Glycoproteins From the Biofouling Diatom Craspedostauros Australis (Bacillariophyceae)," *European Journal of Phycology* 38 (2003): 351–360.

16. A. S. Abdullahi, G. J. Underwood, and M. R. Gretz, "Extracellular Matrix Assembly in Diatoms (bacillariophyceae). v. Environmental Effects on Polysaccharide Synthesis in the Model Diatom, Phaeodactylum tricornutum 1," *Journal of Phycology* 42 (2006): 363–378.

17. R. Xiao and Y. Zheng, "Overview of Microalgal Extracellular Polymeric Substances (EPS) and Their Applications," *Biotechnology Advances* 34 (2016): 1225–1244.

18. K. D. Hoagland, J. R. Rosowski, M. R. Gretz, and S. C. Roemer, "Diatom Extracellular Polymeric Substances: Function, Fine Structure, Chemistry, and Physiology," *Journal of Phycology* 29 (1993): 537–566.

19. G. G. Leppard, "Colloidal Organic Fibrils of Acid Polysaccharides in Surface Waters: Electron-Optical Characteristics, Activities and Chemical Estimates of Abundance," *Colloids and Surfaces A: Physicochemical and Engineering Aspects* 120 (1997): 1–15.

20. P. Verdugo, A. L. Alldredge, F. Azam, D. L. Kirchman, U. Passow, and P. H. Santschi, "The Oceanic Gel Phase: A Bridge in the DOM–POM Continuum," *Marine Chemistry* 92 (2004): 67–85.

21. A. W. Decho, "Microbial Biofilms in Intertidal Systems: An Overview," *Continental Shelf Research* 20 (2000): 1257–1273.

22. I. Yalcin, Z. Hicsasmaz, B. Boz, and F. Bozoglu, "Characterization of the Extracellular Polysaccharide From Freshwater Microalgae Chlorella sp," *LWT-Food Science and Technology* 27 (1994): 158–165.

23. S. Arad, L. Rapoport, A. Moshkovich, et al., "Superior biolubricant From a Species of Red Microalga," *Langmuir* 22 (2006): 7313–7317.

24. U. Passow, "Transparent Exopolymer Particles (TEP) in Aquatic Environments," *Progress in Oceanography* 55 (2002): 287–333.

25. S. Zhang, C. Xu, and P. H. Santschi, "Chemical Composition and 234Th (IV) Binding of Extracellular Polymeric Substances (EPS) Produced by the Marine Diatom Amphora sp," *Marine Chemistry* 112 (2008): 81–92.

26. B. Gügi, T. Le Costaouec, C. Burel, P. Lerouge, W. Helbert, and M. Bardor, "Diatom-Specific Oligosaccharide and Polysaccharide Structures help to Unravel Biosynthetic Capabilities in Diatoms," *Marine Drugs* 13 (2015): 5993–6018.

27. F.-J. Cui, L.-S. Qian, W.-J. Sun, et al., "Ultrasound-Assisted Extraction of Polysaccharides From Volvariella volvacea: Process Optimization and Structural Characterization," *Molecules* 23 (2018): 1706.

28. T.-L. Tao, F.-J. Cui, X.-X. Chen, et al., "Improved Mycelia and Polysaccharide Production of Grifola frondosa by Controlling Morphology With Microparticle Talc," *Microbial Cell Factories* 17 (2018): 1–10.

29. S. Ilvitskaya and A. Chistyakova, "Microalgae in Architecture as an Energy Source," In: *IOP Conference Series: Materials Science and Engineering* (IOP Publishing, 2020), 012010.

30. H. Ayadi, N. Toumi, O. Abid, et al., "Étude qualitative et quantitative des peuplements phyto-et zooplanctoniques dans les bassins de la saline de Sfax, Tunisie," *Revue Des Sciences De L'eau* 15 (2002): 123–135.

31. S. Masmoudi, E. Tastard, W. Guermazi, A. Caruso, A. Morant-Manceau, and H. Ayadi, "Salinity Gradient and Nutrients as Major Structuring Factors of the Phytoplankton Communities in Salt Marshes," *Aquatic Ecology* 49 (2015): 1–19.

32. R. R. Guillard and J. H. Ryther, "Studies of Marine Planktonic Diatoms: I. Cyclotella nana Hustedt, and Detonula Confervacea (Cleve) Gran," *Canadian Journal of Microbiology* 8 (1962): 229–239.

33. E. Sanniyasi, A. P. R. Patrick, K. Rajagopalan, R. K. Gopal, and R. Damodharan, "Characterization and in Vitro Anticancer Potential of Exopolysaccharide Extracted From a Freshwater Diatom Nitzschia palea (Kütz.) W. Sm. 1856," *Scientific Reports* 12 (2022): 22114.

34. J. Hedge, B. Hofreiter, and R. Whistler, *Carbohydrate Chemistry* (New York: Academic Press, 1962): 371–380.

35. O. Lowry, N. Rosebrough, A. L. Farr, and R. Randall, "Protein Measurement With the Folin Phenol Reagent," *Journal of Biological Chemistry* 193 (1951): 265–275.

36. E. G. Bligh and W. J. Dyer, "A Rapid Method of Total Lipid Extraction and Purification," *Canadian Journal of Biochemistry and Physiology* 37 (1959): 911–917.

37. T. Bitter and H. M. Muir, "A Modified Uronic Acid Carbazole Reaction," *Analytical Biochemistry* 4 (1962): 330–334.

38. K. Dodgson and R. Price, "A Note on the Determination of the ester Sulphate content of Sulphated Polysaccharides," *Biochemical Journal* 84 (1962): 106.

39. P. Prieto, M. Pineda, and M. Aguilar, "Spectrophotometric Quantitation of Antioxidant Capacity Through the Formation of a phosphomolybdenum Complex: Specific Application to the Determination of vitamin E," *Analytical Biochemistry* 269 (1999): 337–341.

40. M. S. Blois, "Antioxidant Determinations by the use of a Stable Free Radical," *Nature* 181 (1958): 1199–1200.

41. B. Halliwell, J. M. Gutteridge, and O. I. Aruoma, "The Deoxyribose Method: A simple "test-tube" Assay for Determination of rate Constants for Reactions of Hydroxyl Radicals," *Analytical Biochemistry* 165 (1987): 215–219.

42. G.-C. Yen and H.-Y. Chen, "Antioxidant Activity of Various Tea Extracts in Relation to Their Antimutagenicity," *Journal of Agricultural and Food Chemistry* 43 (1995): 27–32.

43. B. Isaksson, L. Nilsson, R. Maller, and L. Sör´ n, "Postantibiotic Effect of Aminoglycosides on Gram-Negative Bacteria Evaluated by a New Method," *Journal of Antimicrobial Chemotherapy* 22 (1988): 23–33.

44. S. Kim, P. A. Thiessen, E. E. Bolton, et al., "PubChem Substance and Compound Databases," *Nucleic Acids Research* 44 (2016): D1202–D1213.

45. J. Thioulouse and J. Lobry, "Co-Inertia Analysis of Amino-Acid Physico-Chemical Properties and Protein Composition With the ADE package," *Bioinformatics* 11 (1995): 321–329.

46. I. Taylor, D. Paterson, and A. Mehlert, "The Quantitative Variability and Monosaccharide Composition of Sediment Carbohydrates Associated With Intertidal Diatom Assemblages," *Biogeochemistry* 45 (1999): 303–327.

47. B. Smestad, A. Haug, and S. Myklestad, "Production of Carbohydrate by the Marine Diatom Chaetoceros affinis var. willei (Gran) Hustedt. III. Structural Studies of the Extracellular Polysaccharide," *Acta Chemica Scandinavica Series B* 28 (1974): 662–666.

48. L. Parwani, M. Bhatt, and J. Singh, "Potential Biotechnological Applications of Cyanobacterial Exopolysaccharides," *Brazilian Archives of Biology and Technology* 64 (2021): e21200401.

49. G. A. Colusse, J. Carneiro, M. E. R. Duarte, J. C.d Carvalho, and M. D. Noseda, "Advances in Microalgal Cell Wall Polysaccharides: A Review Focused on Structure, Production, and Biological Application," *Critical Reviews in Biotechnology* 42 (2022): 562–577.

50. F. Rossi and R. De Philippis, "Role of Cyanobacterial Exopolysaccharides in Phototrophic Biofilms and in Complex Microbial Mats," *Life* 5 (2015): 1218–1238.

51. D. J. Smith and G. J. Underwood, "Exopolymer Production by Intertidal Epipelic Diatoms," *Limnology and Oceanography* 43 (1998): 1578–1591.

52. N. Staats, B. De Winder, L. J. STAL, and L. R. MUR, "Isolation and Characterization of Extracellular Polysaccharides From the Epipelic Diatoms Cylindrotheca Closterium and Navicula Salinarum," *European Journal of Phycology* 34 (1999): 161–169.

53. D. J. Smith and G. J. Underwood, "The Production of Extracellular Carbohydrates by Estuarine Benthic Diatoms: The Effects of Growth Phase and Light and Dark Treatment," *Journal of Phycology* 36 (2000): 321–333.

54. G. Underwood, D. Paterson, and R. J. Parkes, "The Measurement of Microbial Carbohydrate Exopolymers From Intertidal Sediments," *Limnology and Oceanography* 40 (1995): 1243–1253.

55. J. F. C. De Brouwer and L. J. Stal, "DAILY FLUCTUATIONS OF EXOPOLYMERS IN CULTURES OF THE BENTHIC DIATOMS CYLINDROTHECA CLOSTERIUM AND NITZSCHIA SP. (BACILLARIOPHYCEAE)1," *Journal of Phycology* 38 (2002): 464–472.

56. K. Mopper, K. S. Ramana, and D. T. Drapeau, "The role of surface-active carbohydrates in the flocculation of a diatom bloom in a mesocosm," *Deep Sea Research Part II: Topical Studies in Oceanography* 42 (1995): 47–73.

57. F. C. van Duyl, B. de Winder, A. J. Kop, and U. Wollenzien, "Tidal coupling Between carbohydrate concentrations and bacterial activities in diatom-inhabited intertidal mudflats," *Marine Ecology Progress Series* 191 (1999): 19–32.

58. T. Le Costaouëc, C. Unamunzaga, L. Mantecon, and W. Helbert, "New structural insights Into the cell-wall polysaccharide of the diatom *Phaeodactylum tricornutum*," *Algal Research* 26 (2017): 172–179.

59. N. Bhosle, S. Sawant, A. Garg, and A. Wagh, Isolation and partial chemical analysis of exopolysaccharides from the marine fouling diatom Navicula subinflata. 1995.

60. A. Chiovitti, M. J. Higgins, R. E. Harper, R. Wetherbee, and A. Bacic, "The Complex Polysaccharides of the Raphid Diatom Pinnularia viridis (Bacillariophyceae) 1," *Journal of Phycology* 39 (2003): 543–554.

61. Y. Sun, H. Wang, G. Guo, Y. Pu, and B. Yan, "The Isolation and Antioxidant Activity of Polysaccharides From the Marine Microalgae Isochrysis galbana," *Carbohydrate Polymers* 113 (2014): 22–31.

62. F. Krichen, W. Karoud, A. Sila, et al., "Extraction, Characterization and Antimicrobial Activity of Sulfated Polysaccharides From Fish Skins," *International Journal of Biological Macromolecules* 75 (2015): 283–289.

63. L. Wang, Y. Yao, W. Sang, X. Yang, and G. Ren, "Structural Features and Immunostimulating Effects of Three Acidic Polysaccharides Isolated From Panax quinquefolius," *International Journal of Biological Macromolecules* 80 (2015): 77–86.

64. R. B. A. Kolsi, H. B. Salah, N. Jardak, et al., "Sulphated Polysaccharide Isolated From Sargassum vulgare: Characterization and Hypolipidemic Effects," *Carbohydrate Polymers* 170 (2017): 148–159.

65. T. Vasilieva, A. Sigarev, D. Kosyakov, et al., "Formation of Low Molecular Weight Oligomers From Chitin and Chitosan Stimulated by Plasma-Assisted processes," *Carbohydrate Polymers* 163 (2017): 54–61.

66. G. Ren, L. Xu, T. Lu, and J. Yin, "Structural characterization and antiviral activity of lentinan From Lentinus edodes mycelia Against infectious hematopoietic necrosis virus," *International Journal of Biological Macromolecules* 115 (2018): 1202–1210.

67. J. S. Maciel, L. S. Chaves, B. W. Souza, et al., "Structural characterization of Cold Extracted Fraction of Soluble Sulfated polysaccharide From Red Seaweed Gracilaria birdiae," *Carbohydrate Polymers* 71 (2008): 559–565.

68. Y. Athukorala, K.-N. Kim, and Y.-J. Jeon, "Antiproliferative and Antioxidant Properties of an Enzymatic Hydrolysate From Brown Alga, Ecklonia cava," *Food and Chemical Toxicology* 44 (2006): 1065–1074.

69. M. Hajimahmoodi, M. A. Faramarzi, N. Mohammadi, N. Soltani, M. R. Oveisi, and N. Nafissi-Varcheh, "Evaluation of Antioxidant properties and Total Phenolic Contents of Some Strains of Microalgae," *Journal of Applied Phycology* 22 (2010): 43–50.

70. H. Song, M. He, C. Gu, et al., "Extraction Optimization, Purification, Antioxidant Activity, and Preliminary Structural Characterization of Crude Polysaccharide From an Arctic Chlorella sp," *Polymers* 10 (2018): 292.

71. B. Chen, W. You, J. Huang, Y. Yu, and W. Chen, "Isolation and Antioxidant Property of the Extracellular Polysaccharide From Rhodella Reticulata," *World Journal of Microbiology and Biotechnology* 26 (2010): 833–840.

72. Y.-X. Chen, X.-Y. Liu, Z. Xiao, Y.-F. Huang, and B. Liu, "Antioxidant Activities of Polysaccharides Obtained From Chlorella pyrenoidosa via Different eThanol Concentrations," *International Journal of Biological Macromolecules* 91 (2016): 505–509.

73. H. Qi, Q. Zhang, T. Zhao, et al., "Antioxidant Activity of Different Sulfate Content Derivatives of Polysaccharide Extracted From Ulva pertusa (Chlorophyta) in Vitro," *International Journal of Biological Macromolecules* 37 (2005): 195–199.

74. L. S. Costa, G. P. Fidelis, S. L. Cordeiro, et al., "Biological Activities of Sulfated Polysaccharides From Tropical Seaweeds," *Biomedicine & Pharmacotherapy* 64 (2010): 21–28.

75. F. M. de Moraes, S. C. Trauthman, F. Zimmer, et al., "A Polysaccharide-Based Hydrogel as a Green Platform for Enhancing Transdermal Delivery," *Sustainable Chemistry and Pharmacy* 25 (2022): 100604.

76. M.-C. Kang, S. Y. Kim, Y. T. Kim, et al., "In Vitro and in vivo Antioxidant Activities of Polysaccharide Purified From Aloe Vera (Aloe barbadensis) Gel," *Carbohydrate Polymers* 99 (2014): 365–371.

77. M. Berri, C. Slugocki, M. Olivier, et al., "Marine-Sulfated Polysaccharides Extract of Ulva Armoricana Green Algae Exhibits an Antimicrobial Activity and Stimulates Cytokine Expression by Intestinal Epithelial Cells," *Journal of Applied Phycology* 28 (2016): 2999–3008.

78. G. N. Liberman, G. Ochbaum, S. M. Arad, and R. Bitton, "The Sulfated Polysaccharide From a Marine Red Microalga as a Platform for the Incorporation of Zinc Ions," *Carbohydrate Polymers* 152 (2016): 658–664.

79. S. Mashjoor, M. Yousefzadi, M. A. Esmaeili, and R. Rafiee, "Cytotoxicity and Antimicrobial Activity of Marine Macro Algae (Dictyotaceae And Ulvaceae) From the Persian Gulf," *Cytotechnology* 68 (2016): 1717–1726.

80. Z. Zarai, A. Kadri, I. Ben Chobba, et al., "The in-vitro Evaluation of Antibacterial, Antifungal and Cytotoxic Properties of Marrubium vulgare L. Essential Oil Grown in Tunisia," *Lipids in Health and Disease* 10 (2011): 1–8.

81. B. Fang, P. I. Boross, J. Tozser, and I. T. Weber, "Structural and Kinetic Analysis of Caspase-3 Reveals Role for s5 Binding Site in Substrate Recognition," *Journal of Molecular Biology* 360 (2006): 654–666.

82. N. Wakui, R. Yoshino, N. Yasuo, M. Ohue, and M. Sekijima, "Exploring the Selectivity of Inhibitor Complexes With Bcl-2 and Bcl-XL: A Molecular Dynamics Simulation Approach," *Journal of Molecular Graphics and Modelling* 79 (2018): 166–174.